# Dynamics of a Vapour Bubble inside a Vertical Rigid Cylinder in the Absence of Buoyancy Forces

S. Mehran, S. Rouhi, F.Rouzbahani, E. Haghgoo

Abstract—In this paper, growth and collapse of a vapour bubble generated due to a local energy input inside a rigid cylinder and in the absence of buoyancy forces is investigated using Boundary Integral Equation Method and Finite Difference Method. The fluid is treated as potential flow and Boundary Integral Equation Method is used to solve Laplace's equation for velocity potential. Different ratios of the diameter of the rigid cylinder to the maximum radius of the bubble are considered. Results show that during the collapse phase of the bubble inside a vertical rigid cylinder, two liquid micro jets are developed on the top and bottom sides of the vapour bubble and are directed inward. It is found that by increasing the ratio of the cylinder diameter to the maximum radius of the bubble, the rate of the growth and collapse phases of the bubble increases and the life time of the bubble decreases.

**Keywords**—Vapour bubble, Vertical rigid cylinder, Boundary element method, Finite difference method, Buoyancy forces.

# I. INTRODUCTION

AVITATION bubbles are produced in a liquid flow when the static pressure is below the saturated vapour pressure. These bubbles move with liquid flow and violently collapse in high pressure regions [1]. Violent collapse of the bubbles is believed to be one of the most important parameters in mechanical damage of hydraulic machineries and structures, and beneficial parameter in nanomedisin and some surgery. Dynamics of a vapour bubble generated due to a local energy input in the vicinity of different kinds of surfaces is of significant importance in medicine and industry. Numerical and experimental results have shown that a vapour bubble generated due to a local energy input in the vicinity of a rigid boundary is attracted by the rigid surface. In this case during the collapse phase of the bubble a liquid micro jet is developed on the far side of the bubble from the rigid boundary and is directed towards it [2-4]. Numerical results have also shown that during the growth and collapse of a vapour bubble generated due to a local energy input beneath a

free surface, the vapour bubble have a different behavior. In this case the vapour bubble is repelled by the free surface. During the collapse phase a liquid micro jet is developed on the closest side of the bubble to the free surface and is directed away from it [5-7]. In the case of the pulsation of the vapour bubble near a rigid surface, the impingement of the liquid micro jet to the rigid surface is an important cause of mechanical erosion. Experimental investigations also show that at the end of the collapse phase of the vapour bubble and just before its rebound a shock wave is emitted in the liquid domain. The emission of the shock wave inside the liquid domain is also cause of rigid surface destruction [8].

In this paper dynamics of a vapour bubble inside a vertical rigid cylinder with and without a deposit rib generated due to a high local energy input is numerically investigated by employing the Boundary Integral Equation Method. Different ratios of the rigid cylinder diameter to the maximum radius of the bubble are considered. Numerical study on the behavior of a vapour bubble inside a vertical rigid cylinder is of great importance in medicine and industry.

# II. GEOMETRICAL DEFINITION

The vapour bubble is generated due to a local energy input inside a vertical rigid cylinder. The problem is axisymmetric. The vertical and radial axes are shown in figure 1. The vertical rigid cylinder is assumed as a long pipe.

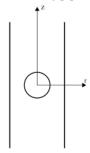


Fig. 1 Schematic representation of the vapour bubble inside a vertical rigid cylinder

# III. HYDRODYNAMIC EQUATION

The liquid flow around the vapour bubble is assumed to be inviscid, irrotational and incompressible and the surface tension is neglected. Therefore the liquid flow around the vapour bubble is a potential flow and the Green's integral formula governs the hydrodynamic behavior of the problem.

S. Mehran is with the Islamic Azad University, Langaroud Branch, P.O.Box 44715-1333, Langaroud, Iran (corresponding author to provide phone: +98-911-139-5265; fax: +98-142-524-4422; e-mail: saeed.mehran2009@gmail.com).

S. Rouhi is with the Islamic Azad University, Langaroud Branch, P.O.Box 44715-1333, Langaroud, Iran (e-mail: saeedroohi2009@gmail.com).

<sup>44715-1333,</sup> Langaroud, Iran (e-mail: saeedroohi2009@gmail.com).
F.Rouzbahani is with the Department of Mechanical Engineering,
University of Tabriz, Tabriz, Iran (e-mail: fardin.roozbahani@gmail.com).

E. Haghgoo is with the Islamic Azad University, Langaroud Branch, P.O.Box 44715-1333, Langaroud, Iran (e-mail: haghgoo926@yahoo.com).

$$C(p)\phi(p) + \int_{S} \phi(q) \frac{\partial}{\partial n} \left[ \frac{1}{|p-q|} \right] dS$$

$$= \int_{S} \frac{\partial}{\partial n} \left[ \phi(q) \left( \frac{1}{|p-q|} \right) dS \right]$$
(1)

where  $\phi$  is velocity potential and S is the boundary of the liquid domain which includes the bubble boundary and the internal surface of the vertical rigid cylinder. p is any point on the boundary or in the liquid domain and q is any point on the boundary. C(p) is  $2\pi$  when p is on the boundary and is  $4\pi$  when p is inside the liquid domain.

The unsteady Bernoulli equation in its Lagrangian form is used for calculating the velocity potential at the successive time steps and is given as

$$\frac{D\phi}{Dt} = \frac{P_{\infty} - P_b}{\rho} + \frac{1}{2} \left| \nabla \phi \right|^2 \tag{2}$$

where  $P_{\infty}$  is pressure in the far field,  $P_b$  is pressure inside the vapour bubble,  $\rho$  is density and t is time.

### IV. DISCRETIZATION OF THE BOUNDARIS

The boundary of the vapour bubble is discretized into M cubic spline elements and the internal surface of the vertical rigid cylinder is divided into 2N linear segments. The origin of the vertical and radial axes is located at the centre of the initial spherical minimum volume of the vapour bubble. The vertical rigid cylinder in both upward and downward of the radial axis is discretized up to physical infinity, where the growth and collapse phases of the vapour bubble have not considerable effects on the fluid flow. Figure 2 illustrates the discretized representation of the vapour bubble generated due to local energy input inside a vertical rigid cylinder without and with a deposit rib. This figure also shows the discretized internal surface of the vertical rigid surface.

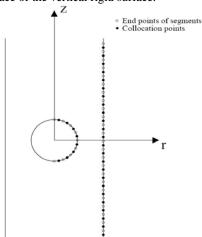


Fig. 2 Discretized representation of the vapour bubble and internal surface of the vertical rigid cylinder in the cases

### V. DISCRETIZATION OF THE EQUATIONS

Equation (3) is a system of linear equations which represents the discretized form of equation (1)

$$2\pi\phi(p_{i}) + \sum_{j=1}^{M+2N} \left\{ \phi(q_{j}) \int_{S_{j}} \frac{\partial}{\partial n} \left[ \frac{1}{|p_{i} - q_{j}|} \right] dS \right\}$$

$$= \sum_{j=1}^{M+2N} \left\{ \frac{\partial}{\partial n} \left[ \phi(q_{j}) \right] \int_{S_{j}} \left( \frac{1}{|p_{i} - q_{j}|} \right) dS \right\}$$
(3)

Whereas equation (4) represents the discretized form of unsteady Bernoulli equation and allows the velocity potential to be time marched over a time increment of  $\Delta t$ .

$$\left[\phi_{i}\right]_{t+\Delta t} = \left[\phi_{i}\right]_{t} + \Delta t \left\{\frac{P_{\infty} - P_{b}}{\rho} + \frac{1}{2}\left|\nabla\phi\right|^{2}\right\}$$
(4)

### VI. EVOLUTION OF THE VAPOUR BUBBLE

A variable time increment is defined as

$$\Delta t = \min \left| \frac{\Delta \phi}{\frac{P_{\infty} - P_c}{\rho} + \frac{1}{2} (\psi^2 + \eta^2)} \right|$$
 (5)

where  $\Delta\phi$  is some constant and represents the maximum increment of the velocity potential between two successive time steps. Also  $P_c$  is saturated vapour pressure,  $\psi$  is normal velocity on the boundary of the liquid domain and  $\eta$  is tangential velocity.

At the beginning of calculations the vapour bubble has a minimum spherical volume with a very high pressure in its inside. Mathematical model for predicting the initial minimum radius of the bubble and the corresponding pressure in its inside is based on the Rayleigh equation [9] which is developed by Best [10]. Details of the calculations for specifying initial values of the bubble volume and its inside pressure is given by Shervani-Tabar et. al. [11]. Normal derivative of the velocity potential and the velocity potential on the bubble boundary at the beginning of the calculations are known and are equal to zero. Also normal velocity on the boundary of the vertical rigid cylinder is known and is equal to zero. Therefore the linear system of equation (3) is solved by employing Gauss elimination method. Consequently the normal velocity on the bubble boundary and the velocity potential on the internal surface of the vertical rigid cylinder are found. By having distribution of the velocity potential on the bubble boundary, the tangential velocity on the bubble boundary is obtained by differentiating the velocity potential on the bubble surface with respect to its arc length. By having normal and tangential velocity on the bubble boundary, radial and vertical components of the velocity on the bubble boundary are obtained. Since the radial and vertical

components of the velocity on the bubble boundary are known, then by employing a second order Runge-Kutta scheme, the evolution of the vapour bubble over a time increment of  $\Delta t$  is obtained. Also by using the discretized form of Bernoulli equation, the distribution of the velocity potential over the bubble surface at the next time step is calculated.

# VII. NONDIMENSIONAL PARAMETERS

The problem under investigation is non-dimensionalized by employing maximum radius of the bubble,  $R_m$ , diameter of the vertical rigid cylinder, D, liquid density,  $\rho$ , pressure in the far field,  $P_{\infty}$  and saturated vapour pressure  $P_c$ . The non-dimensional parameters which are used in this paper are defined as:

$$\lambda = \frac{D}{R_m}, t = \frac{t}{R_m} \left( \frac{P_{\infty} - P_c}{\rho} \right)^{\frac{1}{2}}, \quad \Psi = \psi \left( \frac{\rho}{P_{\infty} - P_c} \right)^{\frac{1}{2}}. \tag{6}$$

### VIII. NUMERICAL RESULTS AND DISCUSSION

Numerical results are obtained in two parts. In part 1 the vapour bubble is generated due to a local energy input inside a vertical rigid cylinder without a deposit rib. While in part 2 the vapour bubble is generated due to a local energy input inside a vertical rigid cylinder with a deposit rib.

Part 1. A vapour bubble inside a vertical rigid cylinder Figure 3 illustrates the growth and collapse phases of a vapour bubble generated due to a local energy input inside a vertical rigid cylinder with  $\lambda = 3$ . Figure 3a shows that the vapour bubble during its growth phase elongates symmetrically in the vertical direction. This phenomenon is due to the effects of the rigid cylinder wall. The rigid cylinder wall prevents the expansion of the bubble in the radial axis and since the top and bottom sides of the bubble are free to move upwards and downwards respectively then the vapour bubble elongates in the vertical direction. Consequently the velocity of the bubble boundary along its top and bottom sides is more than the velocity of the bubble boundary in the vicinity of the rigid cylinder wall. Therefore the fluid particles adjacent to the top and bottom sides of the bubble have greater dynamic pressure with respect to the fluid particles in the vicinity of the rigid boundary. At the end of the bubble growth phase the dynamic pressure in the liquid domain converts to the static pressure. Thus at the early stages of the collapse phase of the bubble the static pressure of the fluid regions adjacent to the top and bottom sides of the bubble is greater than the static pressure of the fluid region between the bubble and the rigid cylinder wall. Therefore during the collapse phase of the bubble the high static pressure on the fluid regions adjacent to the top and bottom sides of the bubble causes development of two broad liquid micro jets on the top and bottom sides of the bubble which are directed inward (as illustrated in fig. 3b).

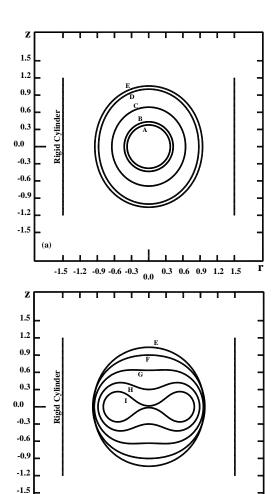


Fig. 3 Growth and collapse of a single vapour bubble inside a vertical rigid cylinder in the absence of buoyancy forces with  $\lambda = 3$ 

0.3 0.6 0.9 1.2 1.5

(a) Growth phase: A)0.00364, B)0.12644, C)0.50345, D)1.42588, E)2.46031,

-1.5 -1.2 -0.9 -0.6 -0.3 0.0

(*b*) Collapse phase: E)2.46031, F)3.09105, G)3.68906, H)4.17126, I)4.51301

Figures 4, 5 and 6 show that by decreasing the ratio of the vertical rigid cylinder diameter to the maximum radius of the bubble,  $\lambda$ , elongation of the vapour bubble during its growth phase in the vertical direction is more appreciable.

A comparison between figure 3 and figure 6 shows that the liquid micro jets in the case of figure 3 are much broader. Thus it should be noted that by increasing  $\lambda$  the liquid micro jets which are developed on the top and bottom sides of the bubble becomes broader. In other words by decreasing  $\lambda$  the effect of the rigid cylinder on the bubble behavior during its growth and collapse phases increases and consequently causes development of two narrower liquid micro jets on the top and bottom sides of the bubble.

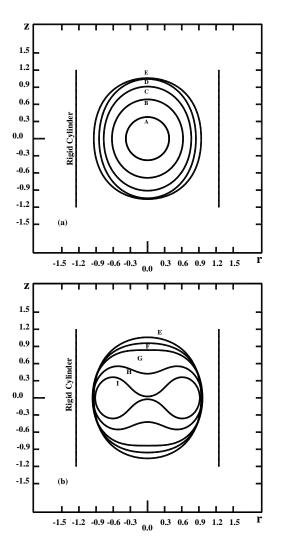


Fig. 4 Growth and collapse of a single vapour bubble inside a vertical rigid cylinder in the absence of buoyancy forces with  $\lambda=2.5$ 

- (a) Growth phase: A)0.00364, B)0.50912, C)1.01104, D)1.51611, E)2.68085,
- (b) Collapse phase: E)2.68085, F)3.11222, G)3.42825, H)4.12248, I)4.63623

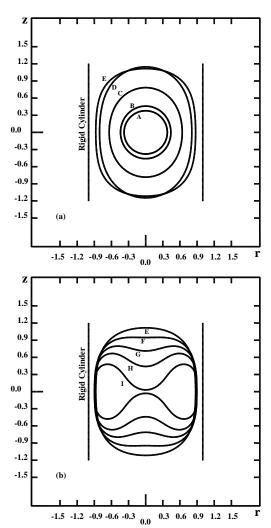


Fig. 5 Growth and collapse of a single vapour bubble inside a vertical rigid cylinder in the absence of buoyancy forces with  $\lambda=2$  (a) Growth phase: A)0.00364, B)0.17783, C)0.67053, D)1.76091, E)2.89102, (b) Collapse phase: E)2.89102, F)3.40912, G)3.85424, H)4.25939, I)4.81757

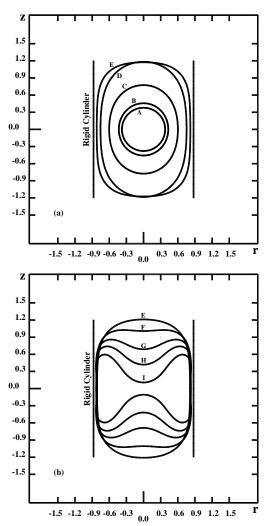


Fig. 6 Growth and collapse of a single vapour bubble inside a vertical rigid cylinder in the absence of buoyancy forces with  $\lambda=1.75$  (a) Growth phase: A)0.00364, B)0.17474, C)0.62814, D)1.65911, E)2.97233, (b) Collapse phase: E)2.97233, F)3.60799, G)4.18045, H)4.57527, I)5.005

Figure 7 shows that by increasing  $\lambda$  the rate of the growth and collapse of a vapour bubble inside a vertical rigid cylinder becomes higher and the life time of the bubble becomes shorter. Therefore by decreasing  $\lambda$  the effect of the rigid cylinder on the behavior of the bubble is more considerable and increase the life time of the bubble.

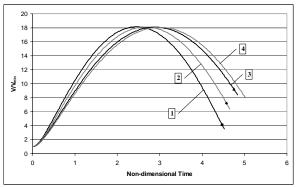


Fig. 7 Variation of rational volume of the bubble in the absence of buoyancy forces against non-dimensional time in the cases of (1)  $\lambda = 3$ , (2)  $\lambda = 2.5$ , (3)  $\lambda = 2$ , (4)  $\lambda = 1.75$ 

Figure 8 illustrates the variation of internal pressure of the vapour bubble inside a vertical rigid cylinder in the cases of figure 7. It should be noted that for the purpose of increasing the life time of the bubble, the pressure at the far field is assumed to be 5000 Pa. This assumption also causes the buoyancy forces to be more appreciable. Numerical study on the dynamics of a buoyant vapour bubble inside a vertical rigid cylinder is our future work.

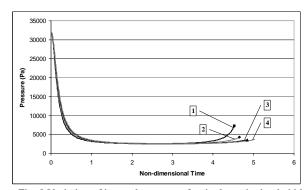


Fig. 8 Variation of internal pressure of a single cavitation bubble inside a vertical rigid cylinder against non-dimensional time in the absence of buoyancy forces in the cases of (1)  $\lambda$  =3, (2)  $\lambda$  =2.5, (3)  $\lambda$  =2, (4)  $\lambda$  =1.75

Figure 9 shows that by increasing  $\lambda$  the velocity of the liquid micro jets at the latest stages of the collapse phase become higher.

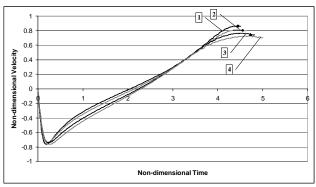


Fig. 9 Variation of non-dimensional velocity of liquid jets in the absence of buoyancy forces against non-dimensional time in the cases of (1)  $\lambda = 3$ , (2)  $\lambda = 2.5$ , (3)  $\lambda = 2$ , (4)  $\lambda = 1.75$ 

Figures 10a illustrates the variation of the pressure at the intersection of the radial axis with the internal surface of the vertical rigid cylinder with respect to non-dimensional time. While figure 10b magnifies the variation of the pressure at the intersection of the radial axis with the internal surface of the vertical rigid cylinder against non-dimensional time at the early stages of the bubble growth phase.

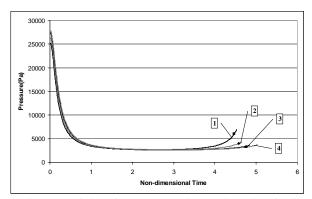


Fig. 10a Variation of pressure at the intersection point of radial axis with internal surface of the vertical rigid cylinder against non-dimensional time in the absence of buoyancy forces in the cases of

(1) 
$$\lambda = 3$$
, (2)  $\lambda = 2.5$ , (3)  $\lambda = 2$ , (4)  $\lambda = 1.75$ 

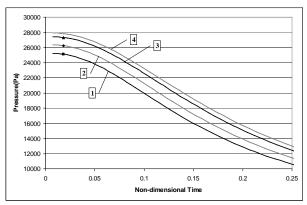


Fig. 10b Variation of pressure at the intersection point of radial axis and internal surface of the vertical rigid cylinder against non-

dimensional time in the absence of buoyancy forces in the cases of (1)  $\lambda = 3$ , (2)  $\lambda = 2.5$ , (3)  $\lambda = 2$ , (4)  $\lambda = 1.75$ 

## IX. CONCLUSION

In this paper dynamic behaviour of a vapour bubble generated due to a local energy input in the absence of buoyancy forces is numerically investigated by employing a Boundary Integral Equation Method.

Numerical results show that the vapour bubble during its growth phase elongates in the vertical direction. During the collapse phase of the bubble two broad liquid micro jets are developed on the top and bottom sides of the bubble and are directed inward.

Results also show that by increasing  $\lambda$ , the ratio of the cylinder diameter to the maximum radius of the bubble, the rate of the growth and collapse of the vapour bubble inside a vertical rigid cylinder becomes higher and the life time of the bubble becomes shorter.

### REFERENCES

- Li, S. C. 2000. "Cavitations of hydraulic machinery," Imperial College Press. pp. 464.
- [2] Blake, J. R., Taib, B. B. and Doherty, G. (1986), "Transient cavities near boundaries; Part 1. Rigid boundary", J. Fluid Mech., Vol. 170, pp. 479-497.
- [3] Blake, J. R. and Gibson, D. C. (1987), "Cavitation bubbles near boundaries", Ann. Rev. Fluid Mech., Vol. 19, pp. 99-123.
- [4] Soh, W. K. and Shervani-Tabar, M. T. (1994), "Computer model for a pulsating bubble near a rigid surface", Computational Fluid Dynamics JOURNAL, Vol. 3, No. 1, pp. 223-236.
- [5] Blake, J. R., Taib, B. B. and Doherty, G. (1986), "Transient cavities near boundaries; Part 2. Free surface", J. Fluid Mech., Vol. 181, pp. 197-212.
- [6] Blake, J. R. and Gibson, D. C. (1981), "Growth and collapse of a vapour cavity bubble near a free surface", J. Fluid Mech., Vol. 111, pp. 123-140.
- [7] Shervani-Tbar, M. T. (1995), "Computer study of a cavity bubble near a rigid boundary, a free surface, and a compliant wall", PhD Thesis, University of Wollongong, Wollongong, Australia.
- [8] Lauterborn, W. (1980), "Cavitation and coherent optics", Cavitation and Inhomogenities in Underwater Acoustics, Proceedings of the First International Conference, , Fed. Rep. of Germany, Lauterborn (Ed.), Springer-Verlag, pp. 3-12.
- [9] Rayleigh, Lord (1917), "On the pressure developed in a liquid during collapse of a spherical void", Phil. Mag., Vol. 34, pp. 94-98.
- [10] Best, J. P. (1991), "The dynamics of underwater explosions", PhD Thesis, University of Wollongong, Wollongong, Australia.
- [11] Shervani-Tabar, M. T., Abdullah, A. and Shabgard, M. R. (2006), " Numerical study on the dynamics of an electrical discharge generated bubble in EDM", Engineering Analysis with Boundary Elements, Vol. 30, pp. 503-514.